European Radiology (2022) 32:4264–4274
https://doi.org/10.1007/s00330-021-08464-x

CHEST

Radiological classification, gene-mutation status, and surgical prognosis of synchronous multiple primary lung cancer

Ji-wen Huo[1] · Tian-you Luo[1] · Xiao-qun He[1] · Jun-wei Gong[1] · Fa-jin Lv[1] · Qi Li[1]

Received: 10 September 2021 / Revised: 19 October 2021 / Accepted: 8 November 2021 / Published online: 6 January 2022
© The Author(s), under exclusive licence to European Society of Radiology 2021

Abstract

Objective To investigate the radiological classification, gene-mutation status, and surgical prognosis of synchronous multiple primary lung cancer (sMPLC).

Methods From January 2013 to October 2019, 192 consecutive patients with sMPLC were investigated. The clinical, CT, molecular, and pathological features of all patients were analyzed. Furthermore, the prognosis of 89 patients who only underwent surgical resection was evaluated.

Results Among 192 patients, all lesions pathologically confirmed or highly suspected as tumors based on radiological findings were retrospectively analyzed, and the CT findings of sMPLC were classified into three types: (I) all lesions manifested as solid nodules/masses (14.06%, 27/192), (II) all lesions manifested as subsolid nodules/masses (43.23%, 83/192), and (III) tumor lesions manifested as a combination of ≥ 2 of the following patterns: solid nodules/masses, subsolid nodules/masses, cystic airspace, and focal consolidation (42.71%, 82/192). For 252 tumors undergoing epidermal growth factor receptor (EGFR)–mutation testing, the EGFR-mutation rate was higher in subsolid tumors than that in solid tumors ($p < 0.05$). Among 19 patients with all tumors undergoing surgery and driver-gene testing, genetic heterogeneity was prevalent among the multiple tumors (63.16%,12/19). The highest clinical stage of non-I, ipsilateral distribution of tumors, and CT classification of I indicated a poor prognosis for patients with sMPLC (all $p < 0.05$).

Conclusion Subsolid lesions are the most common presentation of sMPLC. Genetic heterogeneity in driver mutations among sMPLC may be present. Prognosis in patients with sMPLC is determined by the highest clinical TNM stage, distribution, and radiological classification among the multiple tumors.

Key Points

- *Synchronous multiple primary lung cancer (sMPLC) has three types of CT findings.*
- *Genetic heterogeneity may be prevalent among the multiple tumors.*
- *Prognosis in patients with sMPLC is associated with the highest clinical TNM stage, distribution, and radiological classification among the multiple tumors.*

Keywords Lung neoplasms · Computed tomography · Mutation · Prognosis

Abbreviations

ADC	Adenocarcinoma
CT	Computed tomography
EGFR	Epidermal growth factor receptor
GGO	Ground-glass opacity
IA	Invasive adenocarcinoma
LADC	Lung adenocarcinoma
mMPLC	Metachronous multiple primary lung cancer
MPLC	Multiple primary lung cancer
PACS	Picture archiving and communication system
PFS	Progression-free survival
sMPLC	Synchronous multiple primary lung cancer

✉ Qi Li
lq781222711@163.com

[1] Department of Radiology, the First Affiliated Hospital of Chongqing Medical University, Yuzhong District, No. 1 Youyi Road, Chongqing 400016, China

Introduction

Multiple primary lung cancer (MPLC) is a special type of lung cancer [1]. In 1975, Martini and Melamed first proposed the concept and diagnostic criteria of MPLC and divided it into synchronous multiple primary lung cancer

(sMPLC) and metachronous multiple primary lung cancer (mMPLC) [2]. The term *sMPLC* refers to the synchronous occurrence of two or more primary lung cancers in the same patient, with the diagnostic interval between the two malignant lung tumors being within 6 months. The detection rate of sMPLC has been increasing owing to the development of diagnostic methods and screening procedures over the past decade [3–7].

Computed tomography (CT) is the generally preferred method to localize lesions and provide essential diagnostic information about lung cancer. In clinical practice, tumors in patients with sMPLC exhibit varied appearances on CT images, and the diagnoses may be delayed due to the poor understanding of the imaging findings associated with this condition. In terms of treatment, some recent reports have shown that tumors in patients with sMPLC with different molecular types treated with various methods resulted in better prognoses [8, 9]. Gene-mutation analysis generally requires a sample of the tumor tissue. However, sometimes it is not feasible to acquire adequate tissue samples from all lung lesions because resection of multicentric lesions has some limitations in terms of pulmonary reserve. Some investigators have indicated that CT features of lung cancer in combination with clinical variables can be used to predict the epidermal growth factor receptor (EGFR)-mutation status, but these studies have mainly focused on solitary primary lung cancers [10, 11]. Regarding prognosis, previous studies have reported correlations between the clinical characteristics and surgical prognosis of patients with sMPLC [12–16]. However, only a few studies have examined the relationship between the imaging findings and prognostic factors of patients with sMPLC [15, 16], which has not yet been clarified fully.

Therefore, the present study aimed to thoroughly investigate the radiological classification, gene-mutation status, and surgical prognosis of sMPLC.

Materials and method

Patients

The medical records of all studied patients were retrospectively reviewed. The study was approved by the institutional review board of our institution and the requirement of informed consent was waived due to the retrospective nature of the study. From January 2013 to October 2019, 192 consecutive patients with sMPLC were investigated. All patients underwent CT scanning with ≥ 2 lesions confirmed pathologically by surgical resection, fiberoptic bronchoscopy, or percutaneous puncture. Referring to the concept and diagnostic criteria established by Martini and Melamed in 1975 and supplemented by the American College of Chest Physicians after the twenty-first century [2, 8], the inclusion criteria for sMPLC were as follows: (1) ≥ 2 tumor lesions confirmed with different histological types; for example, adenocarcinoma (ADC) and squamous cell carcinoma. (2) If there were ≥ 2 tumor lesions with the same histological types, they had to meet the following conditions: (a) ≥ 2 tumor lesions located in different pulmonary lobes or segments, bilaterally or unilaterally; (b) no metastasis to the ipsilateral mediastinum or subcarinal lymph nodes (no N2), no metastasis to the contralateral hilar, mediastinum, scalene muscle, or supraclavicular lymph node (no N3), and no extrapulmonary metastasis (no M1). The exclusion criteria were as follows: (1) incomplete imaging data of the patient, (2) tumors with satellite nodules, defined as smaller tumors located close to original cancer in the same segment that usually led to better survival, were not regarded as sMPLC, (3) the patient had a history of chemotherapy, radiotherapy, or other antitumor therapy before CT scanning.

CT image acquisition

Chest CT scanning was performed using a Discovery CT750 HD (GE Healthcare) or Somatom Definition Flash (Siemens Healthcare) scanner. All patients underwent CT scanning in the supine position at the end of inspiration during a single breath-hold. The scanning range included the entire chest from the first rib to the diaphragm. The scanning parameters were as follows: tube voltage, 120 kVp; tube current, 100–250 mA; scan slice thickness/interval for axial images, 5 mm/5 mm. All images were saved in the Picture Archiving and Communication system workstation (Vue PACS, Carestream).

Evaluation of CT features

All images were reconstructed using a section thickness of 0.625–1.25 mm for imaging analysis. Two radiologists with ≥10 years of experience in thoracic radiology blinded to the related clinical data interpreted the axial images on the PACS workstation together. In case of conflicting judgments, a consensus was reached by discussion. For each patient, these lesions that were pathologically confirmed or highly suspected by radiographic evaluation as lung cancer were reviewed. The following data were analyzed and recorded: (1) the number and largest diameter of tumor lesions; (2) distribution (unilateral/bilateral lung); (3) density (solid: tumor without ground-glass opacity (GGO), subsolid: tumor with GGO, including pure GGO and mixed GGO); (4) shape: round, oval, lobulated, or irregular (with an uneven contour that could not be classified as round, oval, or lobulated); and (5) internal characteristics: air bronchogram (air-filled bronchus within the tumor) and airspace (air attenuation within the tumor). After the first interpretation of CT images, the two radiologists decided the radiological

classification criterion through discussion. The radiologists then re-reviewed all CT images and categorized the tumors according to their morphological characteristics.

Identification of epidermal growth factor receptor mutation

Tumor DNA specimens were extracted and analyzed by surgical resection, fiberoptic bronchoscopy, or percutaneous puncture before initiation of the therapy. Genetic mutations were detected using commercially available kits from Amoy Diagnostics. These kits were based on amplification refractory mutation system real-time polymerase chain reaction technology and were used for the qualitative detection and identification of mutations or fusions in EGFR, ALK, BRAF, HER2, KRAS, NRAS, ROS1, PIK3CA, and RET. Each test was performed according to the manufacturer's protocol.

Clinical data and follow-up information

All clinical data were obtained from the electronic medical record system, including the patient's sex, age at first diagnosis of sMPLC, smoking history, date of surgical resection, types of surgical excision, highest clinical stage (defined based on the most extensive tumor in each patient), pathological types, and lymphatic metastasis status. The patient's follow-up information was obtained from outpatient and telephone follow-up. Progression-free survival (PFS) of patients who only underwent surgical resection was calculated from the date of surgery to the time of recurrence or death due to disease progression or to the date of the last follow-up without progression. The last follow-up date was January 5, 2021.

Statistical analysis

Univariate analysis was performed to assess the relationship between CT features and EGFR-mutation status of the tumor lesions using the chi-squared test. The Kaplan–Meier survival analysis and log-rank test were performed to compare the PFSs of patients with different CT and clinical features. Cox proportional hazards regression analysis was performed to determine the prognostic factors. A two-tailed p value of <0.05 was considered to be indicative of statistical significance. All statistical analyses were performed by using the SPSS 25.0 software package (SPSS Statistics 25.0 for Windows).

Results

Basic patient information

A total of 192 patients diagnosed with sMPLC were reviewed, including 101 women (52.60%) and 91 men (47.40%). The average age was 61.85 ± 10.31 years (range, 32–89 years). Furthermore, 114 patients (59.38%) were confirmed to have sMPLC by surgical resection, 45 patients (23.44%) by fiberoptic bronchoscopy, and 33 patients (17.19%) by puncture biopsy. Of the 114 patients with sMPLC who underwent surgery, 108 patients were revisited. Among them, 19 patients who received postoperative adjuvant therapy were excluded, and 89 patients were finally included in the prognostic factor analysis.

Among the 192 patients, 186 patients (96.88%) had lesions that presented the same histological type of ADC, 2 (1.04%) had lesions exhibiting the same histological type of squamous cell carcinoma, and 4 (2.08%) had lesions

Table 1 Basic information of the 192 patients with sMPLC

Clinical features	
Age (years)	61.85 ± 10.31
Sex	
Female	101 (52.60%)
Male	91 (47.40%)
Smoking	
Yes	68 (35.42%)
No	124 (64.58%)
Diagnostic method	
Surgical resection	114 (59.38%)
Fiberoptic bronchoscopy	45 (23.44%)
Puncture biopsy	33 (17.19%)
Highest clinical stage	
I	135 (70.31%)
II	34 (17.71%)
III	23 (11.98%)
Highest pathological stage [a]	
I	74 (83.15%)
II	7 (7.87%)
III	8 (8.99%)
Pathological classification	
Ad + Ad	186 (96.88%)
Sq + Sq	2 (1.04%)
Ad + Sq	3 (1.56%)
Ad + Sc	1 (0.52%)

Ad adenocarcinoma, *Sq* squamous cell carcinoma, *Sc* small-cell lung cancer

[a] The highest pathological stage were not assessed in 103 patients who did not undergo surgical resection

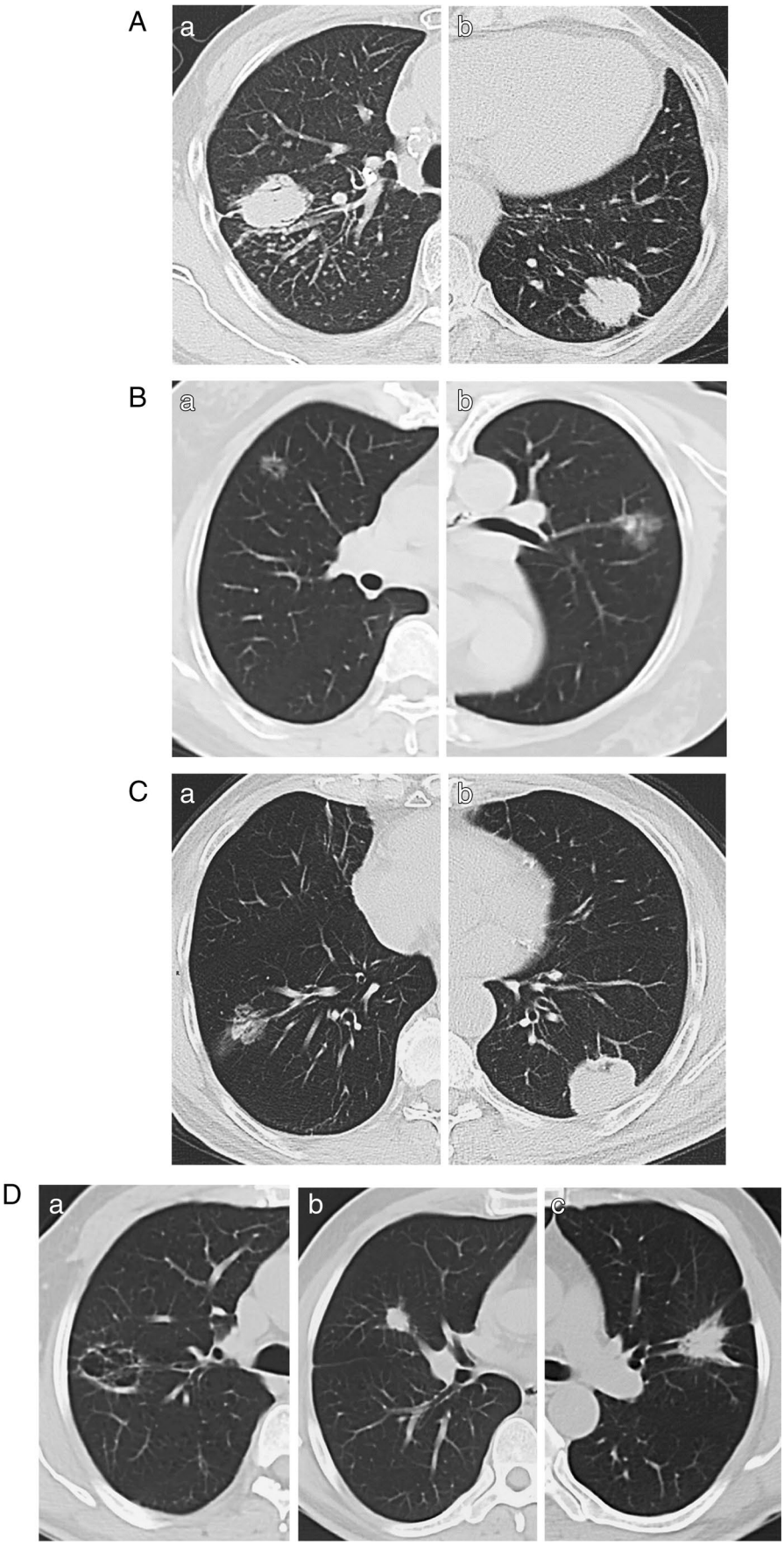

Fig. 1 Computed tomography classification of sMPLC. Axial CT images in the lung window setting of four patients. **A** Patient 1: CT classification of I. A 68-year-old man (a, b), showing a solid nodule with KRAS mutation in the right upper lobe and another solid mass with a wild-type mutation in the left lower lobe. **B** Patient 2: CT classification of II. A 65-year-old woman (a, b), showing a subsolid nodule with 19-Del mutation in the right upper lobe and another subsolid nodule with L858R mutation left upper lobe. **C** Patient 3: CT classification of III. A 71-year-old man (a, b), showing a subsolid nodule with EGFR mutation in the right lower lobe and another solid mass with wild-type mutation in the left lower lobe. **D** Patient 4: CT classification of III. A 54-year-old man (a, b, c), showing cystic airspace with EGFR mutation in the right upper lobe, a solid nodule with wild-type mutation in the right middle lobe, and another focal consolidation with EGFR mutation in the left upper lobe.

exhibiting different histological types. A total of 135 patients (70.31%) had the highest clinical-stage I among the multiple tumors, 34 patients (17.71%) had stage II, and 23 patients (11.98%) had stage III. Out of 89 patients who underwent surgical resection, 74 patients (83.15%) had the highest pathological stage I among the multiple tumors, 7 patients (7.87%) had stage II, and 8 patients (8.99%) had stage III (Table 1).

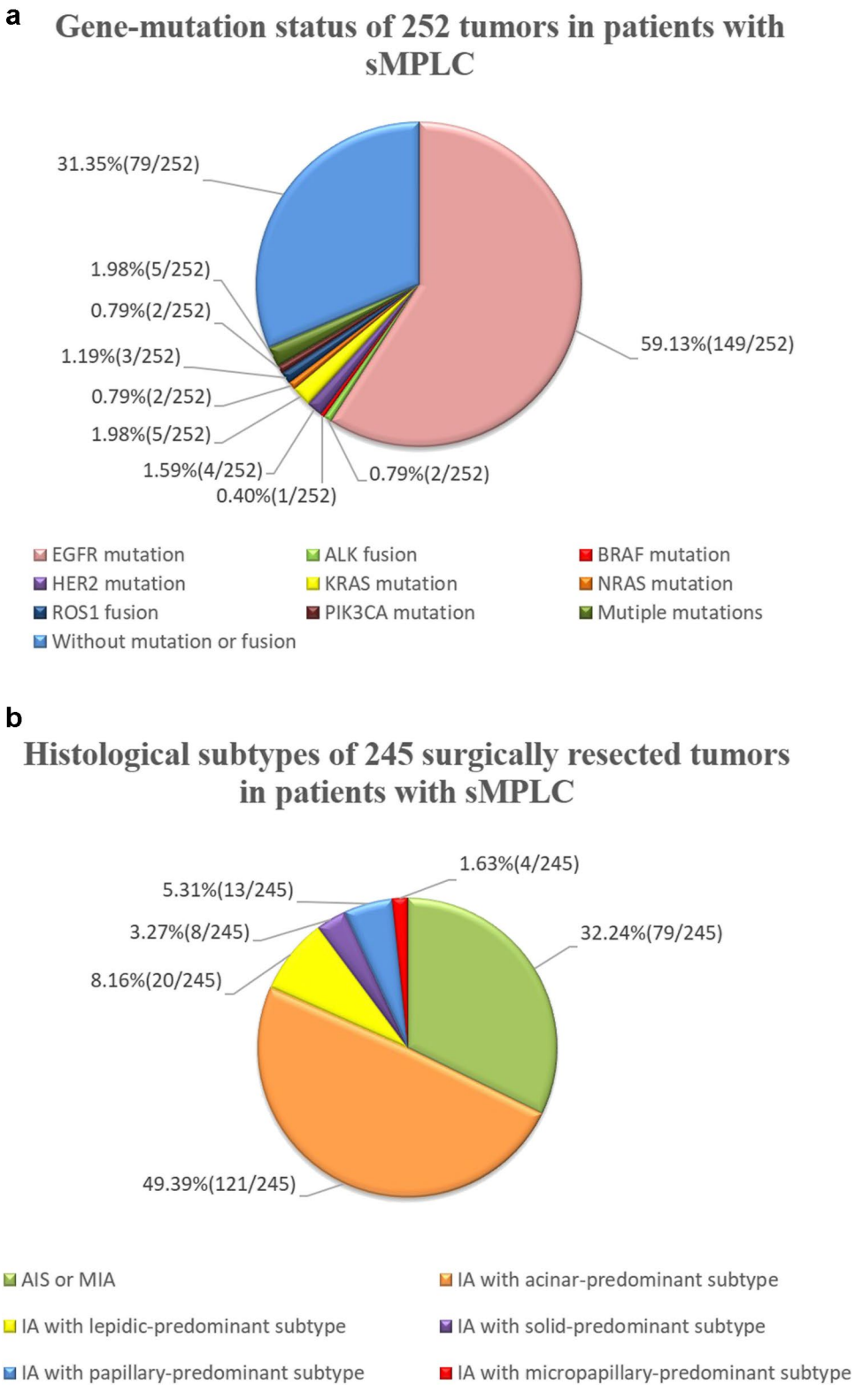

Fig. 2 **a**, **b** Molecular and pathological features of patients with sMPLC. AIS, adenocarcinoma in situ; MIA, minimally invasive adenocarcinoma; IA, invasive adenocarcinoma

CT morphological characteristics and classification

Among the 192 patients, all lesions pathologically confirmed or highly suspected as tumors based on radiological findings were analyzed, and the following four CT findings were established: (1) solid nodule/mass defined as a round or oval opacity with solid density and a diameter measuring up to (nodule) or ≥ 3 cm (mass); (2) subsolid nodule/mass defined as a round or oval opacity with subsolid density and a diameter measuring up to (nodule) or ≥ 3 cm (mass); (3) cystic airspace characterized by a thin-walled cystic airspace; and (4) focal consolidation characterized as a focal consolidation with an irregular shape that could not be classified as round, oval, or lobulated and usually containing air bronchogram.

The sMPLC was actually a mixture of multiple tumors with the different CT findings described above. The CT findings of sMPLC were further classified into the following three types: (I) all lesions manifested as solid nodules/masses (14.06%, 27/192), (II) all lesions manifested as subsolid nodules/masses (43.23%, 83/192), and (III) tumor lesions manifested as a combination of ≥ 2 of the following patterns: solid nodules/masses, subsolid nodules/masses, cystic airspace, and focal consolidation (42.71%, 82/192). Among all patients, 85 (44.27%, 85/192) had a unilateral distribution (27 patients on the left lung, 58 patients on the right lung), and 107 (55.73%, 107/192) had a bilateral distribution (Fig. 1).

Pathological and molecular features

For the 192 patients, a total of 245 lesions were surgically resected. Among them, 79 lesions (32.24%) were confirmed as adenocarcinomas in situ or minimally invasive adenocarcinomas, whereas 166 lesions (67.76%) were confirmed as invasive adenocarcinomas (IAs). For all IAs, acinar-predominant growth patterns were found to be the most common histological subtype for patients with sMPLC, followed by the lepidic-predominant and papillary-predominant patterns (Fig. 2).

A total of 252 lesions had an EGFR mutation and 103 had eight other driver-gene mutations. The specific gene-mutation statuses are depicted in Fig. 2. Among them, 136 lesions (53.97%) were solid nodules/masses, 92 (36.51%) were subsolid nodules/masses, and 24 lesions (9.52%) had two other patterns. The chi-squared test showed that subsolid nodules/masses had a high incidence of EGFR mutations ($p < 0.05$), whereas solid nodules/masses had a low incidence of EGFR mutations ($p < 0.05$) (Table 2).

In 19 patients, surgical resection and nine driver-gene testing were performed for all lesions. For all lesions in the same patient, 12 patients (63.16%) exhibited different gene-mutation statuses, whereas 7 (36.84%) exhibited the same gene-mutation status (Table 3).

Prognostic factor analysis

In total, 89 patients underwent surgical resection alone (average age, 60.48 ± 10.15 years). Among them, 18 patients (20.22%) relapsed and 7 patients (7.87%) died. The Kaplan–Meier survival analysis showed that clinical features, including the highest clinical stage and lymphatic metastasis status, were associated with the PFSs of the patients with sMPLC. The PFS was longer in patients with the highest clinical stage of I than in those with the highest clinical stage of II and III ($p < 0.001$). The PFS was shorter in patients with lymphatic metastasis than in those without ($p < 0.05$). Age, sex, smoking, and surgical resection types were not significantly associated with PFS (all $p > 0.05$). Furthermore, the CT features of tumors, including location, largest tumor size, and CT classification, were correlated with PFS. The PFS was shorter for patients having tumors with ipsilateral distribution than for those having tumors with bilateral distribution, for patients having tumors with the largest tumor size ≥ 3 cm than for those having tumors with the largest tumor size < 3 cm, and for patients with CT

Table 2 Correlation between the CT features and *EGFR*-mutation status of 252 tumors in patients with sMPLC

CT features	Total	*EGFR* positive ($n = 149$)	*EGFR* negative ($n = 103$)	p value
Solid nodule				0.001
Presence	136	68 (50.00%, 68/136)	68 (50.00%, 68/136)	
Absence	116	81 (69.83%, 81/116)	35 (30.17%, 35/116)	
Subsolid nodule				0.001
Presence	92	68 (73.91%, 68/92)	24 (26.09%, 24/92)	
Absence	160	81 (50.63%, 81/160)	79 (49.37%,79/160)	
Cystic airspace/focal consolidation				0.603
Presence	24	13 (54.17%, 13/24)	11 (45.83%, 11/24)	
Absence	228	136 (59.65%, 136/228)	92 (40.35%, 92/228)	

EGFR epidermal growth factor receptor, *CT* computed tomography

Table 3 Genetic-mutation status of 19 patients with sMPLC with all tumors undergoing surgical resection and nine driver-gene testing

Number of patients	Number of lesions	Genetic- mutation status	Lesion 1		Lesion 2		Lesion 3		Lesion 4	
			Mutation or fusion	Location	Mutation or fusion	Location	Mutation or fusion	Location	Mutation or fusion	Location
1	3	S	-	RUL	-	RUL	-	RML		
2	2	S	19Del	LUL	19Del	LUL				
3	2	S	19Del	RUL	19Del	RUL				
4	2	S	19Del	RUL	19Del	RUL				
5	2	S	L858R	RUL	L858R	LUL				
6	2	S	-	RUL	-	LLL				
7	2	S	-	RUL	-	RLL				
8	2	D	-	RUL	L858R	RML				
9	2	D	-	LLL	19Del	LLL				
10	2	D	-	RUL	L858R	RLL				
11	3	D	L868R	RUL	19Del	RLL	-	RLL		
12	4	D	L858R	RUL	19Del	RUL	L858R	RUL	-	RLL
13	2	D	L858R	RUL	-	LUL				
14	2	D	-	LUL	ROS1	RUL				
15	3	D	19Del	LUL	HER2	RLL	L861	RUL		
16	3	D	L858R	LUL	T790M	LUL	ROS1	LUL		
17	2	D	L868R	RUL	19Del	RLL				
18	3	D	L858R	RUL	L858R	RLL	19Del	LLL		
19	2	D	19Del	LUL	L858R	RLL				

S same gene mutation status, *D* different gene mutations status, "-" wild-type mutation, *RUL* right upper lobe, *RML* right middle lobe, *RLL* right lower lobe, *LUL* light upper lobe, *LLL* light lower lobe

classification of I than for those with CT classification of II/III (all $p < 0.05$) (Table 4, Fig. 3).

Cox analysis showed that the highest clinical stage of non-I (hazard ratio (HR) = 7.914, p = 0.000, 95% confidence interval (CI) 2.885–21.708), ipsilateral distribution of tumors (HR = 3.761, $p = 0.019$, 95% CI 1.241–11.400), and CT classification of I (HR = 5.899, $p = 0.001$, 95% CI 2.032–17.127) were independent risk factors associated with the poor prognosis of patients with sMPLC (Table 5).

Discussion

A good understanding of the imaging characteristics and their relationships with gene mutations and the prognosis of sMPLC is of great clinical significance. Therefore, this study comprehensively analyzed the CT classification, gene-mutation status, and surgical prognosis of patients with sMPLC.

Four different CT tumor characteristics were observed: solid nodules/masses, subsolid nodules/masses, cystic airspace, and focal consolidation. Some investigators indicated that sMPLC can manifest as solid/subsolid nodules/masses [15–17], but cystic airspace and focal consolidation were not mentioned in these studies. The two patterns have some special CT presentations. For tumors with thin-walled cystic airspace, the mechanism underlying its formation may be related to focal emphysema resulting from small-airway stenosis due to tumor invasion or intratumoral necrosis [18, 19]. Nonuniform cyst walls, septation within the cyst, wall nodules, GGO around the cyst, and irregular margins are highly indicative of cancer [20]. For tumors with focal consolidation, the air bronchogram finding is usually observed, which can display features similar to those of infection, possibly resulting in diagnostic errors. A dead bronchial leafless tree sign, GGO component, and pleural retraction can indicate cancer. Moreover, the CT findings of sMPLC were

Table 4 Correlation between clinical and CT characteristics and PFS in 89 patients with sMPLC undergoing surgical resection alone

Clinical and CT characteristics	*N* (*n* = 89)	Mean PFS (months)	*p* value
Age (years)			0.556
≥ 65	35 (39.33 %)	44.31 ± 3.23	
< 65	54 (60.67 %)	55.79 ± 4.21	
Sex			0.180
Female	58 (65.17 %)	48.74 ± 4.45	
Male	31 (34.83 %)	60.40 ± 4.04	
Smoking history			0.064
Presence	16 (17.98 %)	42.58 ± 3.35	
Absence	73 (82.02 %)	59.79 ± 3.27	
Highest clinical stage			< 0.001
I	72 (80.90 %)	61.24 ± 3.40	
II	7 (7.87 %)	30.19 ± 3.40	
III	10 (11.24 %)	35.29 ± 7.20	
Surgical resection			0.577
Lobectomy + lobectomy	23 (25.84 %)	39.32 ± 4.10	
Lobectomy + sublobectomy	24 (26.97 %)	53.96 ± 5.40	
Sublobectomy + sublobectomy	42 (47.19 %)	55.47 ± 4.36	
Lymphatic metastasis			0.001
Presence	10 (11.24 %)	32.73 ± 4.43	
Absence	79 (88.76 %)	58.43 ± 3.36	
Largest tumor size			0.006
≥ 3 cm	22 (24.72 %)	36.79 ± 3.36	
< 3 cm	67 (75.28 %)	61.01 ± 3.21	
Tumor location			0.033
Ipsilateral	55 (61.80 %)	48.63 ± 4.67	
Bilateral	34 (38.20 %)	60.49 ± 4.12	
CT classification			
I	9 (10.11 %)	31.56 ± 7.92	0.003
II	47 (52.81 %)	63.56 ± 3.59	
III	33 (37.08 %)	49.15 ± 3.35	

PFS progression-free survival

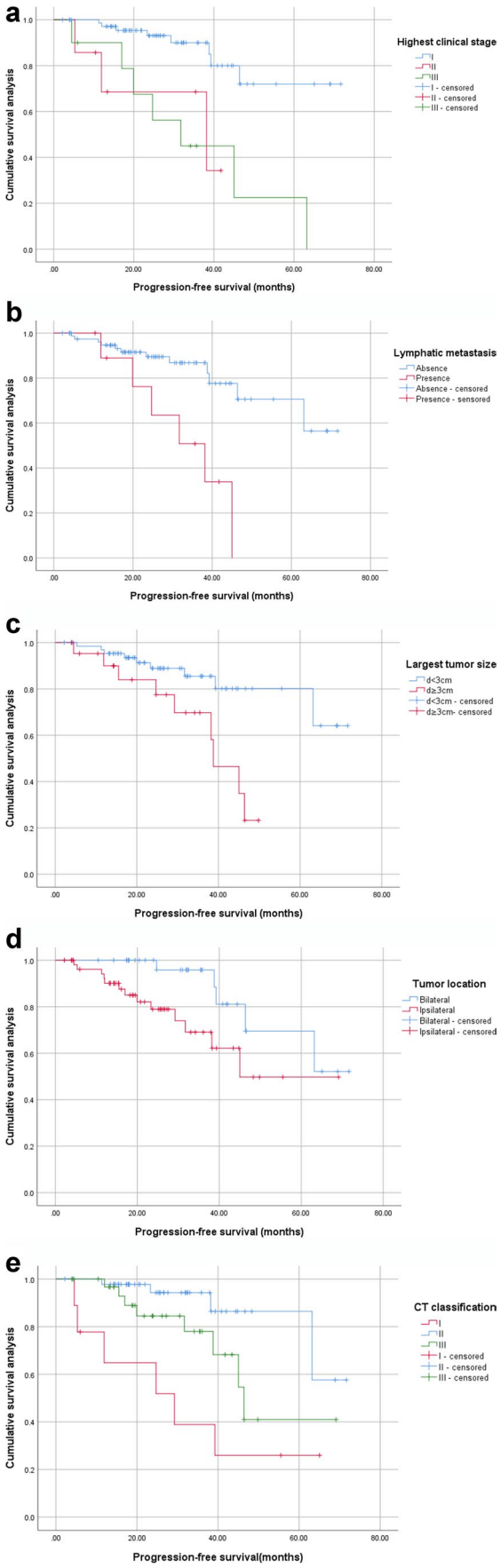

Fig. 3 **a**–**e** Kaplan–Meier survival curve depicting actual progression-free survival in 89 patients with sMPLC undergoing surgical resection alone

further classified into three types. We found that type II, in which all lesions manifested as subsolid nodules/masses, was the most common, followed by type III. Previous studies have reported that the density of tumors was associated with the histological subtype of lung ADC (LADC) [21–23]. LADC with a lepidic-predominant pattern usually presents as a subsolid lesion, whereas predominantly other common patterns (papillary, acinar, solid, and micropapillary) tend to manifest as a solid lesion [21, 22]. This study showed that most tumors in sMPLC were ADC and presented subsolid density features, suggesting that tumors in sMPLC were closely associated with the lepidic-predominant pattern. Familiarity with the overall morphological classification and awareness of the typical CT signs associated with each type will aid clinicians in providing accurate diagnosis and suitable treatment for sMPLC.

We also analyzed the EGFR-mutation status of 252 lesions in sMPLC. The EGFR-mutation rate was higher for subsolid nodules/masses than for solid nodules/masses, corroborating the results of some studies on isolated lung cancer [10, 11, 24, 25]. Furthermore, genetic heterogeneity was prevalent among the multiple tumors. According to the latest American College of Chest Physicians treatment guidelines, radical surgical resection is the optimal treatment for sMPLC [8]. However, a recent case report described a combination of surgery and targeted drugs to treat sMPLC with EGFR gene mutations. In this study, after treatment with gefitinib, the changes in the tumor were compared, and the tumors resistant to gefitinib were surgically removed, whereas those sensitive to gefitinib were continually treated with gefitinib, thereby achieving a better curative effect [9]. A critical question is whether each tumor of sMPLC should be evaluated and treated individually in a similar manner to solitary lung cancer, which warrants further research.

Finally, we identified the prognostic factors of patients with sMPLC who only underwent surgery. Previous studies have reported correlations between lung cancer survival and age, sex, smoking history, tumor distribution, and surgical resection type. Finley et al [14] and El Ghissassi et al [26] found that age, sex, and smoking history were associated with lung cancer survival rates. Conversely, Hattori et al [15, 16] and Shimada et al [27] demonstrated that age, sex, and smoking history were not closely related to PFS, which is consistent with the present study. The different outcomes reported in the literature may be attributed to heterogeneity in patients' basic data and differences in sample sizes. Some investigators [5, 27] indicated that bilateral distribution of tumors predicted poor survival compared with ipsilateral distribution, whereas Tanvetyanon et al [28] and Griffioen

Table 5 Univariate and multivariate survival analysis of prognostic factors in 89 patients with sMPLC undergoing surgical resection alone

Clinical and CT characteristics	Univariate analysis			Multivariate analysis		
	B	HR (95CI%)	*p* value	*B*	HR (95CI%)	*p* value
Highest clinical stage (non-I)	1.811	6.117 (2.400–15.591)	0.000	2.069	7.914 (2.885–21.708)	< 0.001
Lymphatic metastasis (presence)	1.547	4.697 (1.703–12.957)	0.003			
Largest tumor size (D ≥ 3 cm)	1.251	3.494 (1.344–9.084)	0.010			
Tumor location (ipsilateral)	1.099	3.000 (1.045–8.610)	0.041	1.325	3.761 (1.241–11.400)	0.019
CT classification (I)	1.411	4.100 (1.514–11.103)	0.005	1.775	5.899 (2.032–17.127)	0.001

HR hazard ratio, **p* variables in the equation

et al [29] showed that bilateral cancers are indicative of more favorable survival, which corroborates our results. These conflicting results among studies may be attributed to differences in patient inclusion criteria. We speculated that bilateral tumors may have a higher probability of being true MPLC rather than being intrapulmonary metastases. Current diagnostic criteria are inadequate to differentiate sMPLC from intrapulmonary metastasis, especially for the CT classification of type I. Thus, additional studies are needed to improve the criteria. Rostad et al [6] reported that pneumonectomy indicated a poor survival prognosis, whereas Jung et al [30] reported that limited resection was not associated with poor PFS. In the present study, 89 patients received sublobectomy or lobectomy rather than pneumonectomy. Thus, no significant difference between the PFSs of patients with different types of surgical resection was observed. Our results showed that patients with the largest tumor size ≥ 3 cm, lymphatic metastasis, and highest clinical stage of non-I had shorter PFSs. Previous studies have reported similar findings, that smaller sizes of the largest tumor, absence of lymphatic metastasis, and earlier clinical stages indicate a good prognosis in patients with sMPLC [27, 31]. Furthermore, patients with CT classification of I had shorter PFS, whereas those with CT classification of II tended to have a better prognosis. Some studies have indicated that tumors with lepidic-predominant patterns are associated with a good prognosis, whereas acinar/papillary/micropapillary/solid tumors are associated with an intermediate or poor prognosis [22, 31, 32], and that the growth pattern of LADC can show some degree of correlation with tumor density on CT images [21–23]. According to these studies, LADC with solid opacity is strongly associated with an acinar/papillary/micropapillary/solid pattern, whereas that with subsolid opacity is related to a lepidic-predominant pattern. Therefore, our results suggested that patients with sMPLC of type I were prone to relapse and exhibited different biological behavior compared with the others two types. Accordingly, they required an accurate surgical evaluation and close follow-up after surgery.

This study has several limitations. First, we used a single-institution database, which might have introduced data bias. Second, we only included patients with sMPLC, but those without mMPLC, and there was no comparison of the two groups. Third, considering that only a small number of patients received chemotherapy or targeted therapy, we focused on the patients who only received surgical resection in the analysis of prognostic factors, and did not have adequate data to analyze the survival of patients who underwent different treatments in the current study. Hence, future studies are warranted.

In conclusion, subsolid lesions are the most common presentation and genetic heterogeneity in driver mutations among sMPLC may be present. Prognosis in patients with sMPLC is determined by the highest clinical TNM stage, distribution, and radiological classification among the multiple tumors. The highest clinical stage of non-I, ipsilateral distribution of tumors, and CT classification of I are indicative of a poor prognosis in patients with sMPLC.

Funding This study has received funding from the Chongqing Science and Technology Commission (cstc2017jcyjAX0281 and cstc2016shmsztzx10002) and Chongqing Health and Family Planning Commission (2022MSXM147) of China.

Declarations

Guarantor The scientific guarantor of this publication is Qi Li.

Conflict of interest The authors of this manuscript declare no relationships with any companies whose products or services may be related to the subject matter of the article.

Statistics and biometry No complex statistical methods were necessary for this paper.

Informed consent This study and all its protocols were approved by the ethics committee of our institute, written informed consent was not required for this study due to the retrospective nature.

Ethical approval Institutional Review Board approval was obtained.

Methodology

- retrospective
- case-control study
- performed at one institution

References

1. Siegel RL, Fedewa SA, Miller KD et al (2015) Cancer statistics for Hispanics/Latinos, 2015. CA Cancer J Clin 65:457–80
2. Martini N, Melamed MR (1975) Multiple primary lung cancers. J Thorac Cardiovasc Surg 70:606–12
3. Jeudy J, White CS, Munden RF, Boiselle PM (2008) Management of small (3–5-mm)pulmonary nodules at chest CT: global survey of thoracic radiologists. Radiology 247:847–53
4. Warth A, Macher-Goeppinger S, Muley T et al (2012) Clonality of multifocal non-small cell lung cancer: implications for staging and therapy. Eur Respir J 39:1437–42
5. Yu YC, Hsu PK, Yeh YC et al (2013) Surgical results of synchronous multiple primary lung cancers: similar to the stage-matched solitary primary lung cancers? Ann Thorac Surg 96:1966–74
6. Rostad H, Strand TE, Naalsund A, Norstein J (2008) Resected synchronous primary malignant lung tumors: a population-based study. Ann Thorac Surg 85:204–9
7. Nakata M, Sawada S, Yamashita M et al (2004) Surgical treatments for multiple primary adenocarcinoma of the lung. Ann Thorac Surg 78:1194–9
8. Kozower BD, Larner JM, Detterbeck FC, Jones DR (2013) Special treatment issues in non-small cell lung cancer: diagnosis and management of lung cancer, 3rd ed: American College of Chest Physicians evidence-based clinical practice guidelines. Chest 143:e369S-99S
9. Ye C, Wang J, Li W, Chai Y (2016) Novel strategy for synchronous multiple primary lung cancer displaying unique molecular profiles. Ann Thorac Surg 101:e45-7
10. Cao Y, Xu H, Liao M et al (2018) Associations between clinical data and computed tomography features in patients with epidermal growth factor receptor mutations in lung adenocarcinoma. Int J Clin Oncol 23:249–57
11. Liu Y, Kim J, Qu F et al (2016) CT features associated with epidermal growth factor receptor mutation status in patients with lung adenocarcinoma. Radiology 280:271–80
12. Voltolini L, Rapicetta C, Luzzi L et al (2010) Surgical treatment of synchronous multiple lung cancer located in a different lobe or lung: high survival in node-negative subgroup. Eur J Cardiothorac Surg 37:1198–204
13. Fabian T, Bryant AS, Mouhlas AL, Federico JA, Cerfolio RJ (2011) Survival after resection of synchronous non-small cell lung cancer. J Thorac Cardiovasc Surg 142:547–53
14. Finley DJ, Yoshizawa A, Travis W et al (2010) Predictors of outcomes after surgical treatment of synchronous primary lung cancers. J Thorac Oncol 5:197–205
15. Hattori A, Matsunaga T, Takamochi K, Oh S, Suzuki K (2017) Radiological classification of multiple lung cancers and the prognostic impact based on the presence of a ground glass opacity component on thin-section computed tomography. Lung Cancer 113:7–13
16. Hattori A, Takamochi K, Oh S, Suzuki K (2020) Prognostic classification of multiple primary lung cancers based on a ground-glass opacity component. Ann Thorac Surg 109:420–7
17. Aokage K, Miyoshi T, Ishii G et al (2018) Influence of ground glass opacity and the corresponding pathological findings on survival in patients with clinical stage I non-small cell lung cancer. J Thorac Oncol 13:533–42
18. Kim TH, Kim SJ, Ryu YH et al (2006) Differential CT features of infectious pneumonia versus bronchioloalveolar carcinoma (BAC) mimicking pneumonia. Eur Radiol 16:1763–8
19. Li Q, Li X, Li XY, Huo JW, Lv FJ, Luo TY (2020) Spectral CT in lung cancer: usefulness of iodine concentration for evaluation of tumor angiogenesis and prognosis. AJR Am J Roentgenol 215:595–602
20. Li TY (1989) CT diagnosis of pulmonary solitary nodule–a correlative study of CT, X-ray and pathology. Zhonghua Fang She Xue Za Zhi 23:346–9
21. Vazquez M, Carter D, Brambilla E et al (2009) Solitary and multiple resected adenocarcinomas after CT screening for lung cancer: histopathologic features and their prognostic implications. Lung Cancer 64:148–54
22. Moon Y, Lee KY, Park JK (2017) The prognosis of invasive adenocarcinoma presenting as ground-glass opacity on chest computed tomography after sublobar resection. J Thorac Dis 9:3782–92
23. Berry MF, Gao R, Kunder CA et al (2018) Presence of even a small ground-glass component in lung adenocarcinoma predicts better survival. Clin Lung Cancer 19:e47-51
24. Yang Y, Yang Y, Zhou X et al (2015) EGFR L858R mutation is associated with lung adenocarcinoma patients with dominant ground-glass opacity. Lung Cancer 87:272–7
25. Lee HJ, Kim YT, Kang CH et al (2013) Epidermal growth factor receptor mutation in lung adenocarcinomas: relationship with CT characteristics and histologic subtypes. Radiology 268:254–64
26. El Ghissassi F, Baan R, Straif K (2009) A review of human carcinogens–part D: radiation. Lancet Oncol 10:751–2
27. Shimada Y, Saji H, Otani K et al (2015) Survival of a surgical series of lung cancer patients with synchronous multiple ground-glass opacities, and the management of their residual lesions. Lung Cancer 88:174–80
28. Tanvetyanon T, Finley DJ, Fabian T et al (2013) Prognostic factors for survival after complete resections of synchronous lung cancers in multiple lobes: pooled analysis based on individual patient data. Ann Oncol 24:889–94
29. Griffioen GH, Lagerwaard FJ, Haasbeek CJ, Smit EF, Slotman BJ, Senan S (2013) Treatment of multiple primary lung cancers using stereotactic radiotherapy, either with or without surgery. Radiother Oncol 107:403–8
30. Jung EJ, Lee JH, Jeon K et al (2011) Treatment outcomes for patients with synchronous multiple primary non-small cell lung cancer. Lung Cancer. 73:237–42
31. Alam N, Darling G, Shepherd FA, Mackay JA, Evans WK (2006) Postoperative chemotherapy in nonsmall cell lung cancer: a systematic review. Ann Thorac Surg 81:1926–36
32. Ohde Y, Nagai K, Yoshida J et al (2003) The proportion of consolidation to ground-glass opacity on high resolution CT is a good predictor for distinguishing the population of non-invasive peripheral adenocarcinoma. Lung Cancer 42:303–10

Publisher's note Springer Nature remains neutral with regard to jurisdictional claims in published maps and institutional affiliations.